

This article was downloaded by:

On: 22 January 2011

Access details: *Access Details: Free Access*

Publisher *Taylor & Francis*

Informa Ltd Registered in England and Wales Registered Number: 1072954 Registered office: Mortimer House, 37-41 Mortimer Street, London W1T 3JH, UK



The Journal of Adhesion

Publication details, including instructions for authors and subscription information:

<http://www.informaworld.com/smpp/title~content=t713453635>

The Interaction of γ -Glycidoxypropyltrimethoxysilane with Oxidised Aluminium Substrates: The Effect of Drying Temperature

Marie-Laure Abel^a; Acharawan Rattana^a; John F. Watts

^a School of Mechanical and Materials Engineering, University of Surrey, Guildford, Surrey, UK

To cite this Article Abel, Marie-Laure , Rattana, Acharawan and Watts, John F.(2000) 'The Interaction of γ -Glycidoxypropyltrimethoxysilane with Oxidised Aluminium Substrates: The Effect of Drying Temperature', The Journal of Adhesion, 73: 2, 313 – 340

To link to this Article: DOI: 10.1080/00218460008029311

URL: <http://dx.doi.org/10.1080/00218460008029311>

PLEASE SCROLL DOWN FOR ARTICLE

Full terms and conditions of use: <http://www.informaworld.com/terms-and-conditions-of-access.pdf>

This article may be used for research, teaching and private study purposes. Any substantial or systematic reproduction, re-distribution, re-selling, loan or sub-licensing, systematic supply or distribution in any form to anyone is expressly forbidden.

The publisher does not give any warranty express or implied or make any representation that the contents will be complete or accurate or up to date. The accuracy of any instructions, formulae and drug doses should be independently verified with primary sources. The publisher shall not be liable for any loss, actions, claims, proceedings, demand or costs or damages whatsoever or howsoever caused arising directly or indirectly in connection with or arising out of the use of this material.

The Interaction of γ -Glycidoxypropyltrimethoxysilane with Oxidised Aluminium Substrates: The Effect of Drying Temperature*

MARIE-LAURE ABEL, ACHARAWAN RATTANA
and JOHN F. WATTS[†]

*School of Mechanical and Materials Engineering, University of Surrey,
Guildford, Surrey, GU2 7XH, UK*

(Received 6 January 2000; In final form 7 June 2000)

The interaction of γ -glycidoxypropyltrimethoxysilane (GPS) with oxidised aluminium substrates has been investigated in terms of the effect of the drying, or curing, temperature. Samples treated with aqueous solutions of GPS at concentrations of 1,4 and 8% v/v were cured at 25, 50, 93 and 120°C. X-ray photoelectron spectroscopy (XPS) and time-of-flight secondary ion mass spectrometry (ToF-SIMS) were used to construct adsorption isotherms and determine the thicknesses of the various GPS coatings. A temperature effect induces subtle changes in the structure of the resulting films. The uptake of GPS is increasing with increasing concentration of GPS. The structure of the films changes at a threshold temperature between 50 to 93°C. XPS and ToF-SIMS data both indicate that the interaction of the GPS film on aluminium is different for low and high temperatures drying regimes. Using the Beer-Lambert equation, it was found that increasing the curing temperature leads to the variation of the thickness of silane films. This is interpreted in terms of changes in the crosslink density of the films and in their state of hydration and/or degradation.

Keywords: XPS; ToF-SIMS; Organosilane; Aluminium; Cure temperature

* One of a collection of papers honoring F. James Boerio, the recipient, in February 1999, of *The Adhesion Society Award for Excellence in Adhesion Science, Sponsored by 3M*.

[†] Corresponding author. Tel.: 44-1483-300 800, Fax: 44-1483-259 508, e-mail: j.watts@surrey.ac.uk

1. INTRODUCTION

Organosilanes are extensively used as adhesion promoters in order to enhance the adhesion of organic coatings and adhesives to metal surfaces [1]. They are widely employed in many applications, particularly the aerospace industries [2]. The general formula of organosilanes is $R'Si(OR)_3$ where R' and R represent an organofunctional and a hydrolysable group, respectively [1, 3]. The interaction of various organosilane molecules with metallic substrates, using adsorption isotherms and XPS, was investigated for the first time by Castle and Bailey [4]. They showed that the chemisorption undergone by the silane molecules followed the Tempkin form. More specifically, γ -glycidoxypropyl trimethoxy silane (GPS) interaction with iron oxide was investigated by Gettings and Kinloch and by Davis and Watts using both XPS and ToF-SIMS. They concluded that there was formation of a covalent bond (Fe–O–Si) between the oxide of steel or iron and the GPS molecule [5, 6]. In the case of aluminium, various researchers brought evidence of the formation of a similar covalent bond [7–9] between aluminium oxide and organosilanes (Al–O–Si). But it is only recently that it was shown unambiguously by Abel *et al.*, using very high mass resolution ToF-SIMS [10]. The interaction of

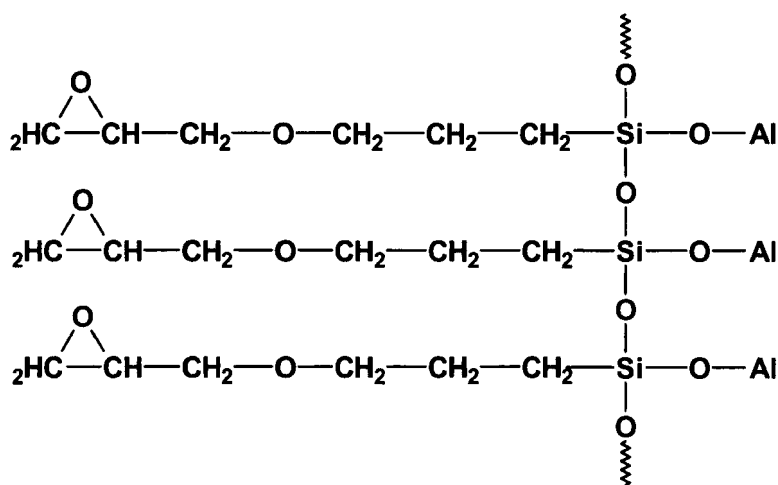


FIGURE 1 Schematic of GPS monolayer on aluminium substrate.

GPS molecules with aluminium when forming a monolayer is illustrated in Figure 1.

The effect of many variables on the interaction of a particular organosilane with a substrate has been studied extensively. These include parameters such as the pH of the solution [11–13], hydrolysis time, silane concentration [1, 3], type of solvent [14] and surface pretreatment [15, 16]. Initial work by Mazza [16] and further investigation by Digby *et al.* [2] have identified the optimum process parameters to provide highest levels of strength and durability. The solution chemistry of the process has been comprehensively investigated by Bertelsen and Boerio [17, 18]. However, the studies of these variables do not lead to a complete understanding of their respective effect. Therefore, in this work, one of these variables which to date has received little attention in the literature, the effect of the curing temperature, was investigated.

2. MATERIALS AND EXPERIMENTAL METHODS

2.1. Materials

The aluminium substrate supplied by Goodfellows Cambridge Ltd., was of high purity (99.99%). The alumina used for grit-blasting was supplied by Abrasive Developments Ltd. The silane, γ -glycidoxypropyltrimethoxysilane (GPS), was of high purity and supplied by OSi Silquest (product designation A187). The water employed was of MilliQ grade (reverse osmosis deionised and carbon filtered). The brushes were made of natural hair, supplied by BDH. Acetone and isopropanol used for rinsing the substrate were also supplied by BDH and were of spectroscopic grade.

2.2. Preparation of the Samples

The aluminium sheet was cleaned with soapy water and rinsed with tap and deionised water, followed by acetone. It was then grit-blasted with 50 μm alumina. Sample discs of 10 mm diameter were punched from the aluminium sheet. Finally, the aluminium samples were degreased with isopropanol, in order to remove any particulate material from grit-blasting and the punch.

2.3. Silane Treatment

Three solutions (25 cm^3) of GPS were prepared: 0.25 cm^3 , 1 cm^3 and 2 cm^3 aliquots of GPS were mixed with MilliQ water to produce 1%, 4% and 8% (v/v) solutions, respectively. The solutions were left for an hour to reach full hydrolysis [17,19]. The grit-blasted aluminium samples were then coated by brushing the GPS solution for two minutes and then left to drain vertically for a short while. The samples were dried at four different curing temperatures at each concentration for an hour. The curing temperatures were as follows: room temperature ($\sim 25^\circ\text{C}$), 50°C , 93°C and 120°C . The set of experiments performed for this study is summarized in Table I.

2.4. Surface Analysis

2.4.1. X-ray Photoelectron Spectroscopy (XPS)

XPS spectra were recorded using a VG Scientific ESCALAB MKII spectrometer. The analysis area was $5 \times 2\text{ mm}^2$. A $\text{MgK}\alpha$ source with an energy of 1253.6 eV was used, at a power of 200 W . The take-off angle was set at 45° for all samples. Survey spectra were recorded together with the core levels and Auger transitions of interest: C1s, O1s, Al2p, Si2p, SiKLL, Na1s and Ca2p. Quantification and peak fitting were carried out using a VGS 5000S data system based on a DEC PDP 11/73 computer interfaced to the spectrometer. The analyser was operated in the constant analyser energy mode at a pass energy of 100 eV for the survey spectra and a pass energy of 50 eV for high-resolution spectra. A quantitative surface analysis was obtained using the peak areas of the high-resolution spectra, following background removal, and the appropriate atomic sensitivity factors.

TABLE I Matrix of experiments

GPS concentration (% v/v)	Temperature of drying ($^\circ\text{C}$)			
	25	50	93	120
1	✓	✓	✓	✓
4	✓	✓	✓	✓
8	✓	✓	✓	✓

2.4.2. Calculation of a Silane Film Thickness

In XPS, there are two well-established approaches to gaining an insight into near surface (up to ca. 6 nm) concentration gradients. The first is angle-resolved XPS (ARXPS) in which the analyses are recorded at electron take-off angles varying from grazing to normal emission. The second is to change the kinetic energy of the core level of interest, an option which is conveniently achieved by switching from $MgK\alpha$ to $AlK\alpha$ radiation or *vice versa*. Unfortunately, neither option is applicable in the current work. A rough surface, such as one that has been blast cleaned, is unsuitable for ARXPS, and the use of achromatic $AlK\alpha$, which would increase the analysis depth by 1–2 nm, cannot be used because of the superposition of a Bremsstrahlung-induced $AlKLL$ Auger peak and the $Si2p$ photoelectron line in this radiation. A monochromated $AlK\alpha$ source was not available. In order to enable comparisons to be made between the various samples, an approach involving the use of the Beer–Lambert equation has been employed to calculate an equivalent silane overlayer thickness as described below.

The thickness of a silane coating on the aluminium surface can be calculated using the Beer–Lambert equation, as follows:

$$I_{Al}^d = I_{Al}^{\infty} \exp(-d/\lambda \sin \theta) \quad (1)$$

where

I_{Al}^d is the intensity of $Al2p$ electrons emitted attenuated by a silane layer of thickness d (nm),

I_{Al}^{∞} is the intensity of electrons from an infinitely thick, clean aluminium substrate,

θ is the electron take-off angle relative to the sample surface,

λ is the inelastic mean free path of the $Al2p$ electrons (nm).

The Beer–Lambert equation can be transformed as shown below for the case of a reduced thickness overlayer:

$$I_{Si2p}^d = I_{Si2p}^{\infty} [1 - \exp(-d/\lambda \sin \theta)] \quad (2)$$

Hence, the thickness of silane, d , is expressed by

$$d = -\lambda \sin \theta \ln \left[1 - \frac{I_{Si2p}^d}{I_{Si2p}^{\infty}} \right] \quad (3)$$

where

λ is the inelastic mean free path of the Si2p electrons (nm),
 $\lambda_{\text{Si}} = 2.5$ nm.

I_{Si2p}^d is the intensity of Si2p signal emitted from an overlayer thickness,
 d .

I_{Si2p}^∞ is the intensity of Si2p signal from an infinitely thick film of
 silane.

2.4.3. Time-of-flight Secondary Ion Mass Spectrometry (ToF-SIMS)

ToF-SIMS analysis was achieved using a VG Scientific Type 23 system, equipped with a two-stage reflectron time-of-flight analyser and a MIG300P pulsed liquid metal ion source. Static SIMS conditions were employed using a pulsed 20 keV, $^{69}\text{Ga}^+$ primary ion beam rastered over a frame area of 500×500 square micrometres. The system was operated using a pulse width of 25 ns, and a beam current of 1.0 nA. The mass range of analysis was $m/z = 5$ to 600 in both positive and negative ion modes.

Relative peak intensities (RPI) were obtained from the following formula:

$$\text{RPI}_x = \frac{I_x}{I_{\text{Total}}} \quad (4)$$

where the subscript x identifies the ion of interest and I_{Total} is the integrated ion intensity between $m/z = 5$ to 300.

3. RESULTS

3.1. Aluminium Substrate

Figure 2 shows the survey spectrum of a grit-blasted aluminium sample. Al2p, Al2s, Si2p, Si2s, C1s, CKLL, Ca2p, Ca2s, CaLMM, O1s, OKLL and NaKLL signals are present. Calcium and sodium signals and a very weak silicon signal originate from the grit transferred to the sample during the blast cleaning operation (the bulk concentration of the grit was obtained from Abrasive Developments Ltd., and is shown in Tab. II). Table III shows the surface concentration in

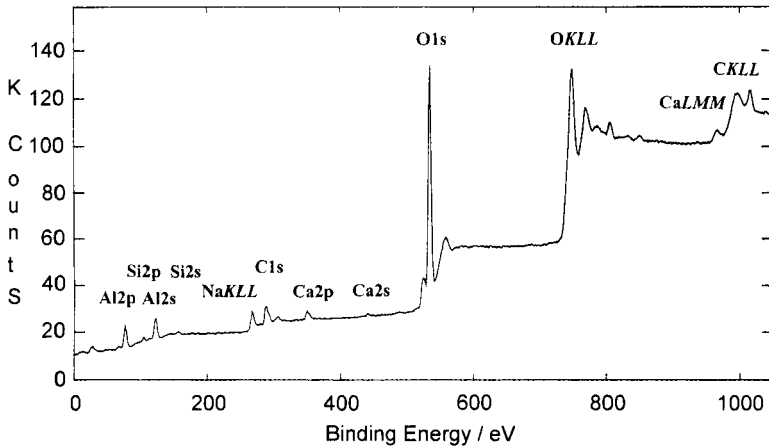


FIGURE 2 XPS survey spectrum of grit-blasted aluminium.

TABLE II Composition of the grit used for grit-blasting

Materials	Bulk concentration (wt %)
Al ₂ O ₃	balance
SiO ₂	0.02
Fe ₂ O ₃	0.03
TiO ₂	0.01 maximum
CaO	0.01
Na ₂ O	0.2
K ₂ O	0.01 maximum

TABLE III Surface concentration for grit-blasted aluminium

Samples	Surface concentration (atomic %)					
	C	O	Al	Si	Na	Ca
Grit-blasted aluminium ¹	16.3	58.3	19.6	2.4	2.0	1.4
Grit-blasted aluminium ²	18.2	63.9	16.1	1.7	*	*

¹ Grit-blasted aluminium for samples cured at room temperature and 50°C.

² Grit-blasted aluminium for samples cured at 93°C and 120°C.

* Below detection limit.

atomic % of the grit-blasted aluminium used for samples cured at room temperature and 50°C and for samples cured at 93°C and 120°C. The surface concentration of the carbon is very low indicating a very clean surface with very little adventitious carbon. The oxygen concentration is high as a result of oxide formation in the atmosphere.

Figure 3 shows a positive ToF-SIMS spectrum in the mass range of $m/z = 0$ to 240 for the grit-blasted aluminium. Masses 23 and 40 are assigned to Na^+ and Ca^+ ions. Mass 27 can be assigned to either Al^+ or C_2H_3^+ ions, although it is very likely to be dominated by Al^+ given the high intensity, and the low concentration of carbon indicated by XPS. This assumption is confirmed by the relatively low intensity of ions that may be assigned to hydrocarbon in the immediate vicinity of mass $m/z = 27$ such as $m/z = 29$ (C_2H_5^+), $m/z = 41$ (C_3H_5^+) and $m/z = 43$ (C_3H_7^+). Other ions are apparent and most of them originated from hydrocarbon contamination as follows: C_4H_9^+ , C_6H_5^+ , $\text{C}_6\text{H}_{13}^+$, $\text{C}_7\text{H}_{15}^+$, $\text{C}_9\text{H}_{19}^+$ and $\text{C}_{11}\text{H}_{17}^+$ for ions of $m/z = 57$, 85, 99, 127 and 149, respectively. Mass 71 can be assigned to either gallium ion ($^{71}\text{Ga}^+$) from the ion beam or $\text{C}_5\text{H}_{11}^+$. Other ions, such as 77, 91, 105, 115, 128 and 141 are present, and can be assigned to aromatic structures. These are thought to arise from the pumping and grit-blasting systems. Alternative assignments for the previously mentioned fragments are possible as they may also originate from plasticizers released from the polymeric water storage container. For example, di-isooctyl phtalate exhibits masses at 149 but also at 57, 71, 77 and 99 [20]. In this case, no C_8 hydrocarbon chain was observed in the spectrum but both C_9 and C_7 can be seen at $m/z = 127$ and 99, respectively. Therefore, the pendant hydrocarbon chain from the plasticizer may be of a chain of seven carbons with a side chain of two carbons. This would also partly explain the presence of aromatic ions on the surface.

3.2. Silane Treatment

Figures 4a to c show the survey spectra of grit-blasted aluminium treated with GPS solutions (1%, 4% and 8%) and dried at 50°C, respectively. The surface concentration of elements is similar to that of grit-blasted aluminium apart from silicon which increases and oxygen which decreases slightly for the sample treated with 1% GPS solution. The silicon signal increases with initial solution concentration, relative to the aluminium signals and the oxygen concentration has dropped slightly. The surface concentration of various samples treated with silane solutions is given in Table IV. Sodium and calcium are present

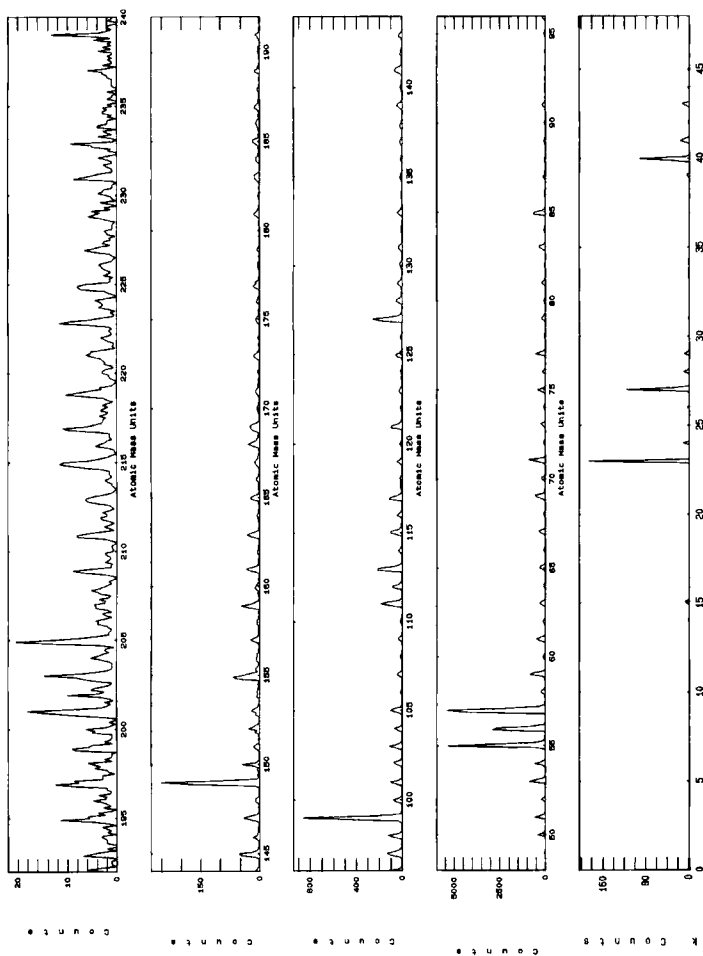


FIGURE 3 Positive ToF-SIMS spectrum in the mass range of $m/z = 0$ to 240 of grit-blasted aluminium.

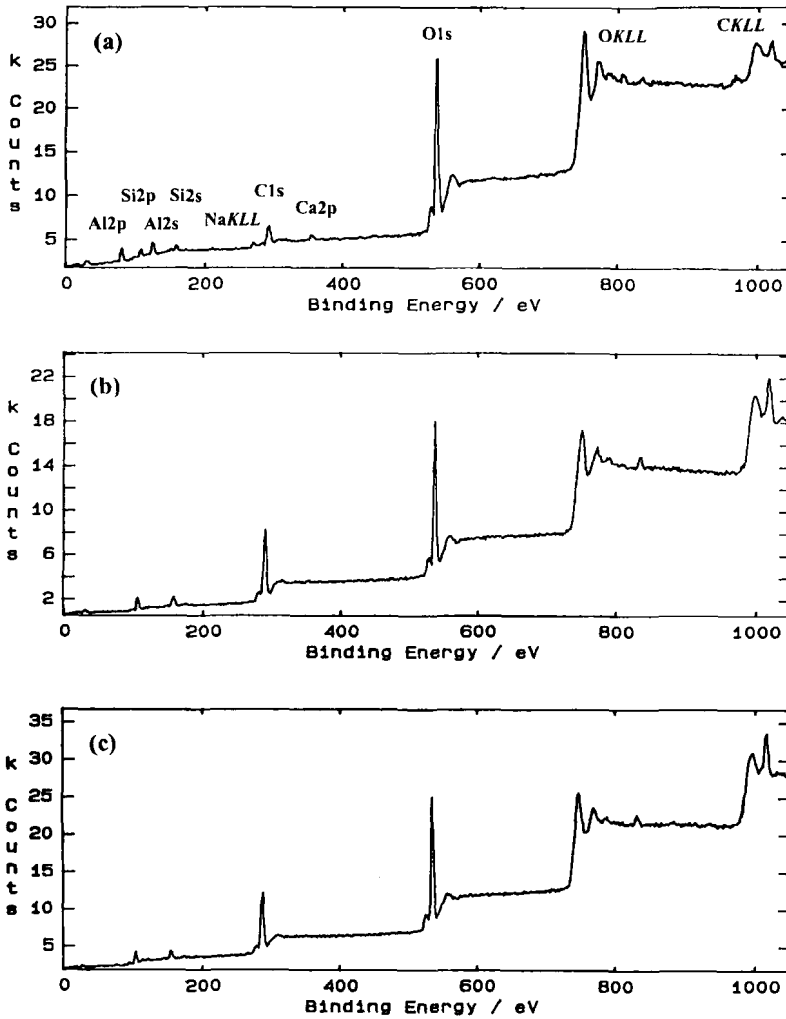


FIGURE 4 XPS survey spectra of grit-blasted aluminium treated with (a) GPS at 1% (v/v); (b) 4% (v/v); (c) 8% (v/v); dried at 50°C.

as a result of the grit-blasting but there is no systematic change in their concentrations. This is presumably a result of their diffusion through the silane film layer [21]. Aluminium is not detected for some of the samples, mainly those coated with the higher concentration GPS solutions. This is because the film thickness exceeds the depth of XPS

TABLE IV Surface concentration for samples treated with GPS

Sample treatment		Surface concentration (atomic %)					
Temperature (°C)	Concentration of GPS (v/v)	C	O	Al	Si	Na	Ca
RT	1%	39.3	44.4	7.1	6.8	0.2	*
	4%	39.1	47.4	5.0	7.7	0.4	0.4
	8%	49.8	43.2	*	7.0	*	*
50	1%	18.3	59.0	16.4	4.6	0.8	0.8
	4%	55.8	40.1	*	3.9	*	0.2
	8%	51.2	38.8	1.9	7.8	*	0.2
93	1%	31.5	51.3	9.2	5.3	0.4	2.3
	4%	33.3	47.0	11.1	6.2	0.4	2.0
	8%	51.2	41.4	*	7.1	*	0.3
120	1%	41.7	40.6	8.8	6.3	0.7	1.8
	4%	45.2	41.9	6.1	6.8	*	*
	8%	55.3	34.0	1.0	9.5	*	0.2

* Below detection limit.

analysis for this particular take-off angle ($\theta = 45^\circ$), namely, 5 to 6 nanometers.

A comparison of the surface composition of the grit-blasted samples with the silane-treated samples indicates that the carbon signal is increasing whereas the aluminium and oxygen signals decrease when the samples are coated with GPS. This shows an increase of organic material on the aluminium surfaces and, therefore, a retention of GPS on the aluminium oxide surface.

Figure 5 presents the uptake of GPS *versus* the initial concentration of GPS in the solution as a plot of the silicon surface concentration; *i.e.*, an adsorption isotherm [22]. It can be seen that two types of curves are obtained for films dried at room temperature or 50°C, 93°C and 120°C, respectively. The curve obtained at room temperature shows an increase of silicon concentration *versus* GPS concentration that tends to plateau at 4% (v/v). The other temperatures exhibit an increase in silicon concentration that does not reach any plateau. This may indicate a different structure for the two families of curves but also that a temperature threshold exists from one type to another above room temperature.

Thicknesses of the various silane films were calculated according to Eq. (3). They are reported in Table V. The apparent thickness decreases as a function of increasing temperature and this effect is more obvious for the 4% (v/v) solution. In the case of samples

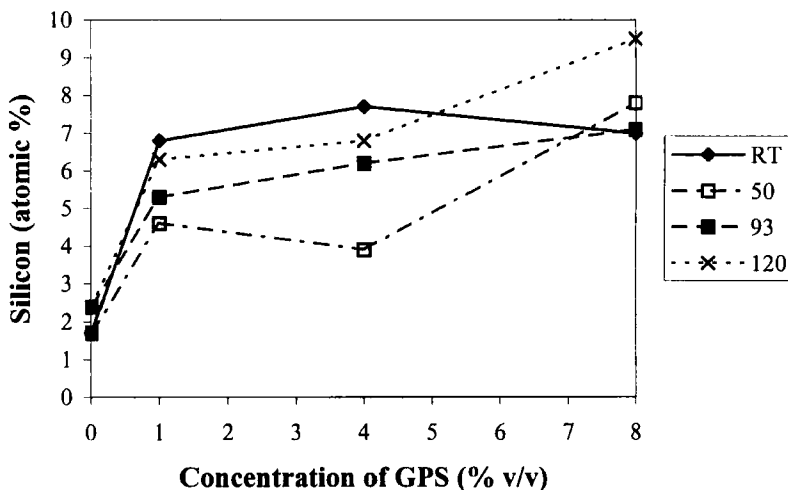


FIGURE 5 Uptake of GPS silane by XPS *versus* initial solution concentration of GPS silane in the solution.

TABLE V Apparent thickness of silane coatings

Concentration of GPS	Thickness of silane, nm			
	RT	50°C	93°C	120°C
1%(v/v)	2.9	1.8	2.0	0.8
4%(v/v)	3.9	1.1	0.8	0.3
8%(v/v)	*	*	*	0.9

* Thickness of the film > 7.5 nm.

prepared with 8% GPS solution, only one thickness value was available for a temperature of drying set at 120°C. This again shows a decrease in thickness compared with samples dried at the lower temperature for which thicknesses are not available, as the films formed exceed the sampling depth of XPS analysis. Figure 6 shows this behaviour as a function of temperature; the GPS film is thicker at room temperature if a solution at 4% is used rather than 1%. When the temperature of drying is increased the trend is reversed, and the films prepared with 1% are always thicker than those prepared at higher concentration.

Figures 7a to c show the positive ToF-SIMS spectra in the mass range of $m/z = 0 - 240$ of aluminium samples treated with GPS at 1, 4

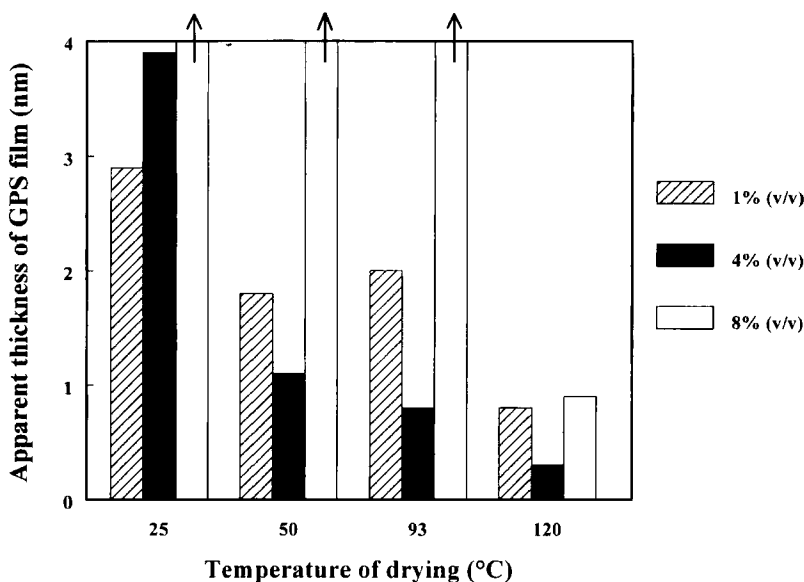


FIGURE 6 Equivalent thickness of silane films as a function of temperature and solution concentration.

and 8% and dried at room temperature, respectively. Fragments characteristic of GPS are reported in Table VI. Fragments at $m/z = 27$ and 28 are assigned to aluminium $^{27}\text{Al}^+$ and silicon $^{28}\text{Si}^+$. It should be noted that $m/z = 28$ is very intense in these spectra, which indicates that the GPS films are not highly crosslinked. Some common silicone oil contamination is present, although not intense, and fragments such as $m/z = 73$, 147 and 207 are assigned to polydimethyl siloxane (PDMS) [20, 23]. Sodium exhibits only one fragment as it has only one isotope and is present at $m/z = 23$. Its intensity decreases with GPS initial concentration in line with the film thicknesses reported in Table V. Fragments present at $m/z = 60$ and 61, although of low intensity, can be assigned to SiO_2^+ and SiO_2H^+ . All specimens exhibit very clear fragments at masses 57, 71, 121, 133 and 181. They are all characteristic of GPS either from the epoxy end or the silanol and/or of the entire molecule. Fragment $m/z = 57$ is assigned to the epoxy side of GPS. Fragment $m/z = 71$ can be assigned to various signals mostly characteristic of GPS and, although these assignments are discussed in detail elsewhere [10], they are included with the other fragments in

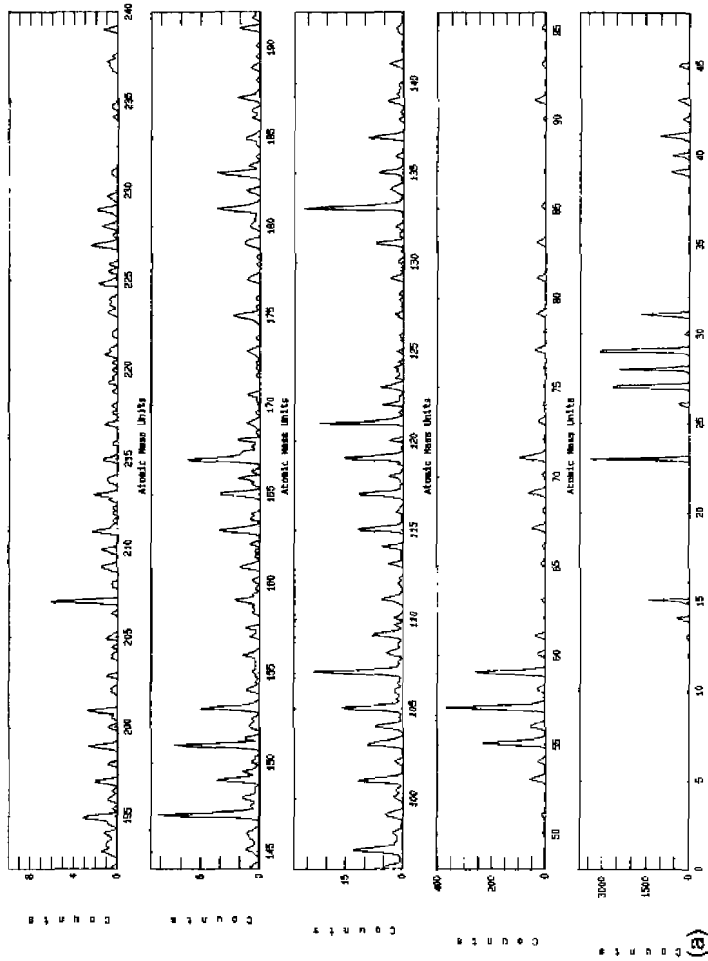


FIGURE 7 Positive ToF-SIMS spectra in the mass range of $m/z = 0$ to 240 of grit-blasted aluminium treated with GPs at (a) 1% (v/v); (b) 4% (v/v); (c) 8% (v/v); dried at room temperature.

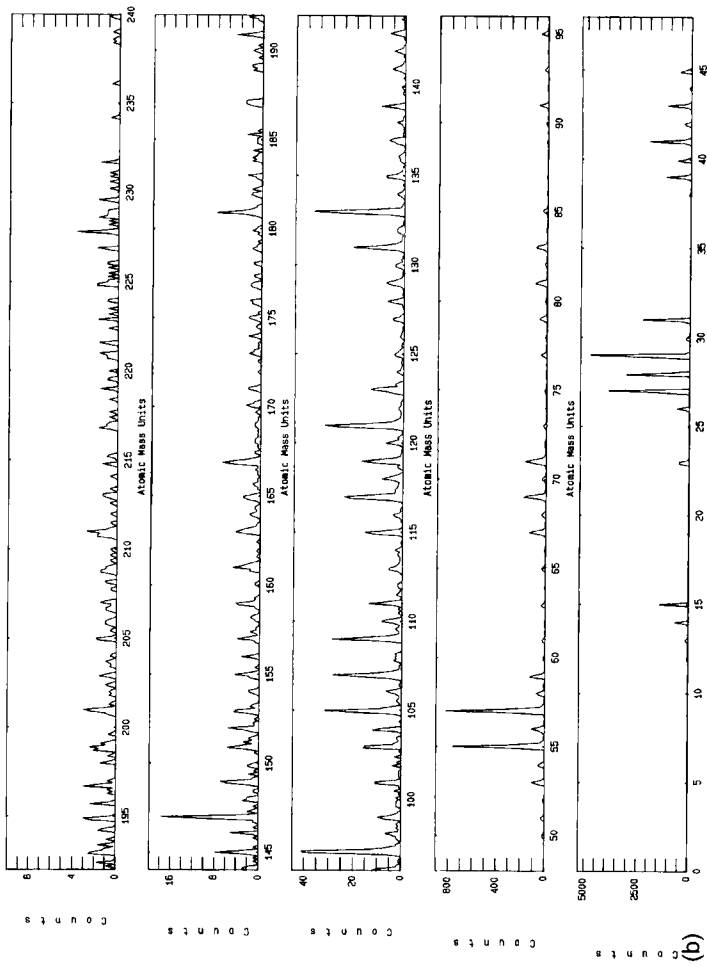


FIGURE 7 (Continued).

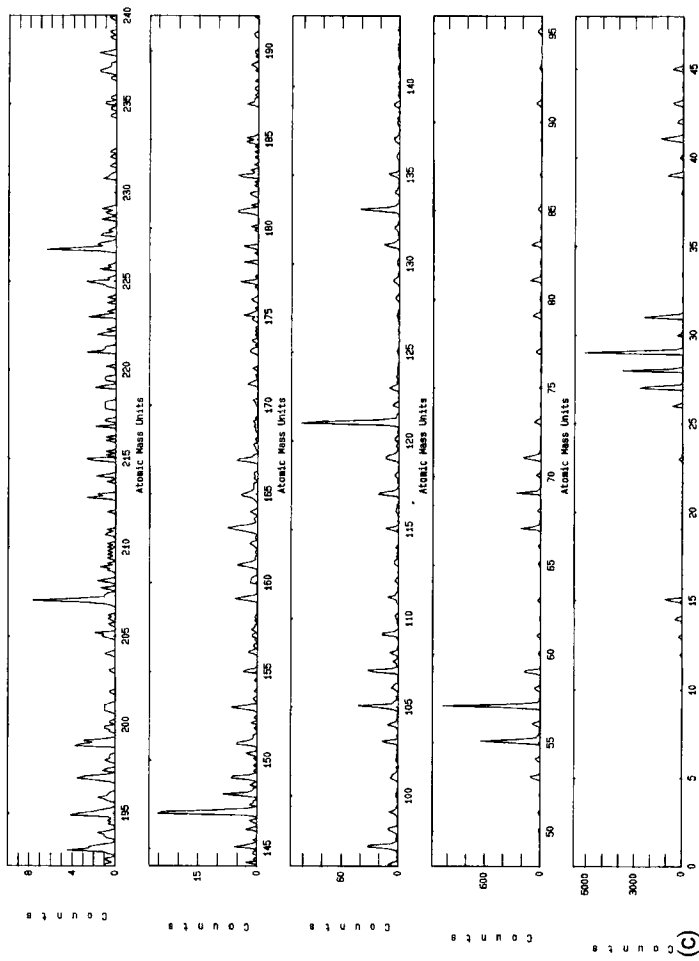


FIGURE 7 (Continued).

TABLE VI Fragments present in the positive and negative modes of detection for samples treated with GPS

m/z	Formula for positive ions	Formula for negative ions	Structure
28	$^{28}\text{Si}^+/\text{C}_2\text{H}_4^+/\text{CO}^+$		
57	$\text{C}_3\text{H}_5\text{O}^+$		$\text{H}_2\text{C}-\overset{\text{O}}{\underset{\text{O}}{\text{CH}}}-\text{CH}_2^+$
71	$\text{SiOAl}^+/\text{SiOC}_2\text{H}_5^+$ $\text{C}_3\text{H}_7^+/\text{C}_4\text{H}_7\text{O}^+/\text{C}_3\text{H}_2\text{O}_2^+$		$\text{Al}-\text{O}-\text{Si}^+$ $\text{CH}_2=\text{CH}-\text{Si}^+=\text{O}$
73	$\text{Si}(\text{CH}_3)_3^+$		
77		SiO_3H^-	$\begin{array}{c} \text{OH} \\ \\ \text{Si}-\text{OH} \\ \\ \text{O}^- \end{array}$
79	$\text{Si}(\text{OH})_3^+$		$\begin{array}{c} \text{OH} \\ \\ \text{Si}^+-\text{OH} \\ \\ \text{OH} \end{array}$
107	$\text{Si}_2\text{H}_3\text{O}_3^+$		$\begin{array}{c} \text{H}-\text{Si}-\text{O}-\text{Si}^+-\text{H} \\ \quad \\ \text{O} \quad \text{OH} \end{array}$
121	$(\text{CH}_2)_3\text{Si}(\text{OH})_3^+$ $(\text{SiO}_2)_2\text{H}^+$	$\text{C}_3\text{H}_9\text{SiO}_3^-$ $\text{Si}_2\text{O}_4\text{H}^-$	$\begin{array}{c} \text{OH} \\ \\ \text{Si}^+-\text{O}-\text{Si} \\ \quad \\ \text{O} \quad \text{O} \end{array} \quad \begin{array}{c} \text{OH} \\ \\ \text{CH}_2-\text{CH}_2-\text{CH}_2-\text{Si}-\text{OH} \\ \\ \text{OH} \end{array}$ $\begin{array}{c} \text{O}^- \\ \\ \text{CH}_3-\text{CH}_2-\text{CH}_2-\text{Si}-\text{OH} \\ \\ \text{OH} \end{array} \quad \begin{array}{c} \text{H} \quad \text{O}^- \\ \quad \\ \text{Si}-\text{O}-\text{Si} \\ \quad \\ \text{O} \quad \text{O} \end{array}$
133	$\text{C}_4\text{H}_{13}\text{OSi}_2^+$		$\begin{array}{c} \text{CH}_3 \quad \text{CH}_3 \\ \quad \\ \text{CH}_2 \quad \text{CH}_2 \\ \quad \\ \text{H}-\text{Si}-\text{O}-\text{Si}-\text{H} \\ \quad \\ \text{H} \quad \text{H} \end{array}$
137	$\text{C}_3\text{H}_9\text{SiO}_4^-/\text{Si}_2\text{O}_5\text{H}^-$		$\begin{array}{c} \text{OH} \\ \\ \text{O}^--(\text{CH}_2)_3-\text{Si}-\text{OH} \\ \\ \text{OH} \end{array} \quad \begin{array}{c} \text{OH} \quad \text{O}^- \\ \quad \\ \text{Si}-\text{O}-\text{Si} \\ \quad \\ \text{O} \quad \text{O} \end{array}$

TABLE VI (Continued)

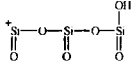
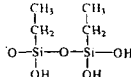
<i>m/z</i>	<i>Formula for positive ions</i>	<i>Formula for negative ions</i>	<i>Structure</i>
181	$(\text{SiO}_2)_3\text{H}^+$		
197		$\text{C}_4\text{H}_{13}\text{Si}_2\text{O}_5^-$	

Table VI. The peak at $m/z = 121$ can be assigned to fragments characteristic of the hydrolysed GPS molecule alone or to a partial crosslinking of two silane molecules. The latter argument is also valid for 181, but in this case for three silane molecules. Fragment $m/z = 133$ is also characteristic of PDMS although it is too intense in the spectra from these samples to be assigned to PDMS only. Moreover, other specimens clearly demonstrated contamination from PDMS in this study but did not exhibit a strong signal at $m/z = 133$. This is an indication that this fragment does not arise from contamination but from GPS and, as shown in Table VI, it can be assigned to partial crosslinking of GPS involving three oxygen atoms in the structure. Spectra obtained in the negative SIMS mode are not presented here as very little variation is seen, but the corresponding fragments are also reported in Table VI.

Figures 8a to d present the positive ToF-SIMS spectra in the mass range of $m/z = 0$ to 240 of aluminium samples treated with GPS at 4% (v/v) then dried at room temperature, 50°C, 93°C and 120°C, respectively. At room temperature and 50°C, similar fragments to those described above are obtained. When the temperature is increased, contamination fragments obtained on the surface after grit-blasting are seen again which indicates that the thickness of the GPS film decreases. This is in agreement with thickness values reported in Table V. This indicates also that the hydrocarbon contamination is not displaced from the aluminium surface when GPS is deposited. These spectra also show that the sodium signal is increasing, together with the calcium and aluminium signals, which is again an indication that the thickness of the film decreases with temperature.

Figures 9a to e show the plot of the relative peak intensity of fragments characteristic of GPS and of $^{23}\text{Na}^+$ which is used to provide

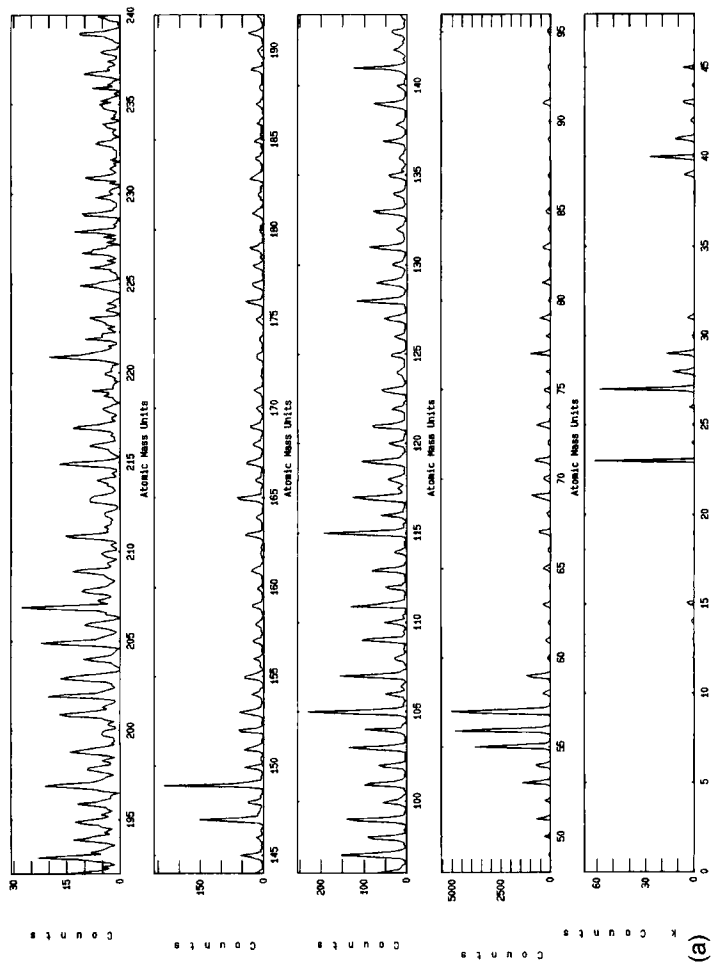


FIGURE 8 Positive ToF-SIMS spectra in the mass range of $m/z = 0$ to 240 of grit-blasted aluminium treated with GPS at 4% (v/v) then dried at (a) room temperature; (b) 50°C; (c) 93°C; (d) 120°C.

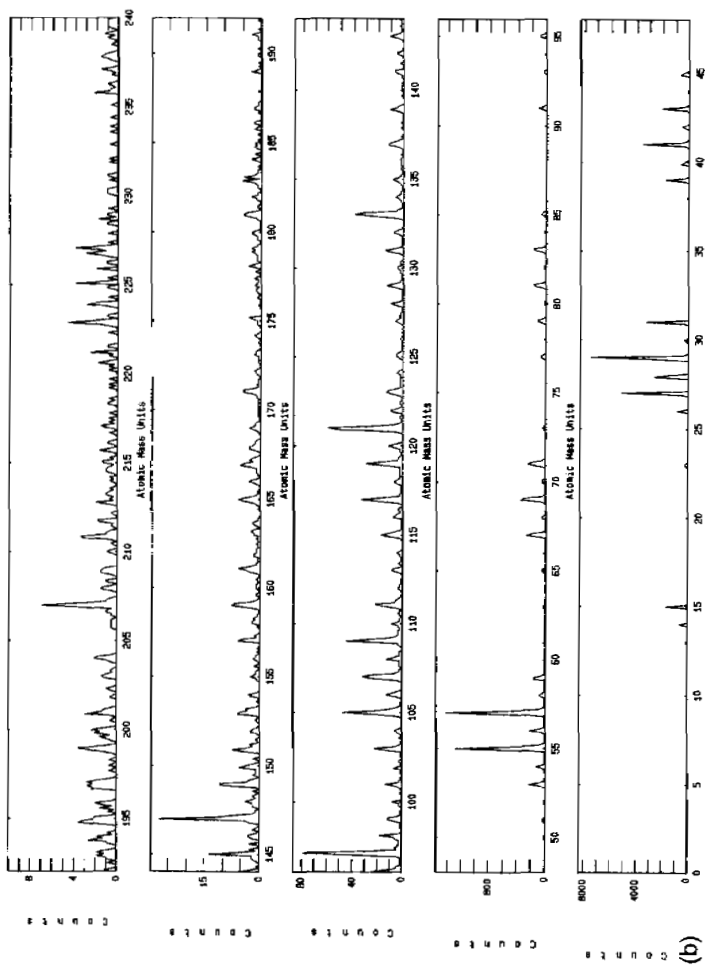


FIGURE 8 (Continued).

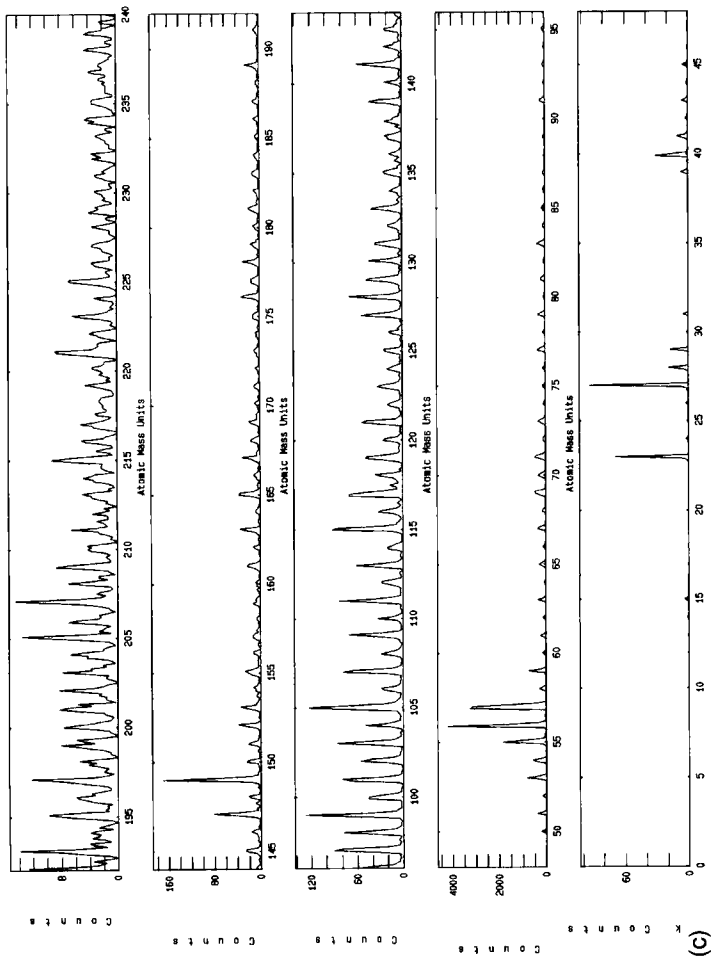


FIGURE 8 (Continued).

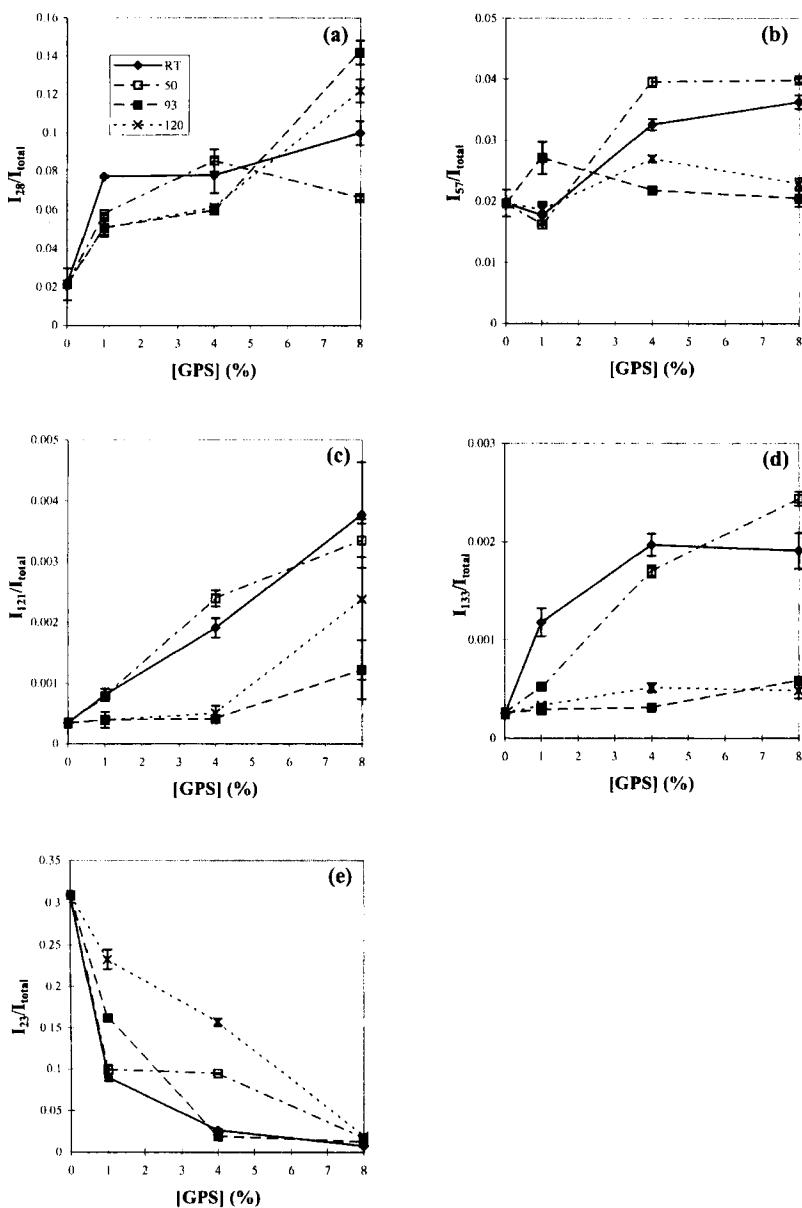


FIGURE 9 Positive ToF-SIMS plot of relative peak intensities versus GPS concentration for the following fragments: (a) $m/z = 28$ (Si^+); (b) $m/z = 57^+$ (epoxy); (c) $m/z = 121^+$; (d) $m/z = 133^+$; (e) $m/z = 23^+$ (Na^+).

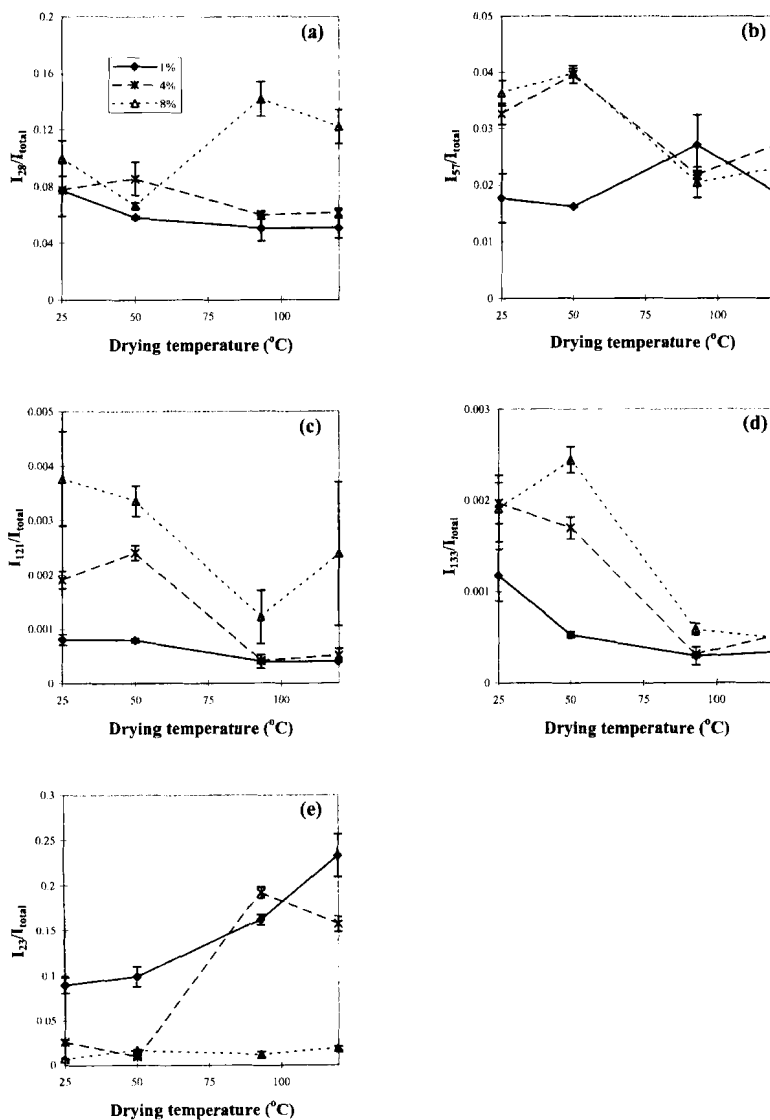


FIGURE 10 Positive ToF-SIMS plot of relative peak intensities *versus* temperature of drying for the following fragments: (a) $m/z = 28$ (Si^+); (b) $m/z = 57^+$ (epoxy); (c) $m/z = 121^+$; (d) $m/z = 133^+$; (e) $m/z = 23^+$ (Na^+).

an unambiguous, high cross-section marker of the substrate. These figures have been plotted as RPIs *versus* initial GPS solution concentration. A close examination allows the classification of the curves obtained in two different groups. For example, the curves obtained for the fragments $m/z = 121$ and $m/z = 133$ demonstrate two different forms of curve for the low temperatures and high temperatures treatments, respectively. In the same manner, the fragment $m/z = 28$ (Si^+) exhibits two types of behaviour with room temperature and 50°C reaching a plateau in intensity, whereas the samples dried at 93°C and 120°C demonstrate a constant increase in relative concentration. The effect is less visible on the $m/z = 57$ fragment, although two types of curves are seen again for initial concentrations of GPS above 1%. The intensity of fragment $m/z = 23$ (Na^+) decreases as a function of GPS concentration indicating that the substrate is attenuated by the GPS overlayers. This clearly indicates differences in the respective ion yields resulting from the drying temperature. Figures 10a to e show the same relative peak intensities plotted as a function of drying temperature. Examination of the various curves for fragments characteristic of GPS demonstrates a decrease in intensity in almost all cases. The curves obtained for $m/z = 23$ all increase, but for samples prepared at a GPS concentration of 8% this is in line with a decrease of the GPS films thicknesses on drying. It should also be noted that most specimens prepared at a GPS concentration of 8% exhibit thick films which totally attenuate the $^{23}\text{Na}^+$ signal in the ToF-SIMS analysis. This is consistent with the XPS data; indeed, it is now well established that, in SIMS, atomic ions have an analysis depth comparable with XPS, *i.e.*, much deeper than the more surface-sensitive fragment ions.

4. DISCUSSION

The increase of cure temperature appears to have various effects on the resulting film: an increase of the crosslink density and degradation of the deposited film; we also assume that elevated temperature will eliminate, in part or totally, the amount of water enclosed in the film,

particularly at temperatures over 100°C, as well as methanol formed during hydrolysis.

Various authors have shown that elevating the temperature of drying increases the crosslink density of a silane film. Dilligham and Boerio, using reflection-absorption infra-red spectroscopy (RAIRS) [24], reported a change in the crosslink density of silane primer films prepared from a 50:50 molar ratio of aminosilane and phenyltrimethoxysilane after drying at 100°C for one hour. They also noticed a decrease in the intensity of the methoxy stretching vibration band which they partly assigned to evaporation of unpolymerized material [24]. This may also be due to evaporation of methanol contained in the film. Both effects would result in the decrease of a silane film thickness. A comparison of the silicon surface concentration for all samples (Tab. IV, Fig. 5) indicates that all samples treated with 1% GPS solution exhibit a lower concentration of silicon than the film dried at room temperature. The same trend is observed for all specimens treated with 8 and 4% GPS solution concentration. A similar evaporation effect was reported by Mishra and Weimer [25]. They showed that clean copper samples placed in the same oven as silane coated samples would exhibit Si2p peaks characteristic of silane, whereas those dried on their own in the same oven would not. This is in agreement with a hypothesis of GPS film degradation during the curing process. It also appears that the crosslink density increases. This is indicated by the observation that the integrated intensity for the whole ToF-SIMS spectrum decreases as the cure temperature is increased. This only occurs for the samples prepared at 93°C and 120°C. The total intensities obtained for samples prepared with 1% and 4% (v/v) cured at 93 and 120°C yield average values of 403702 and 230940 counts for 1% and 452390 and 385453 counts for 4%, for the lower and higher cure temperatures, respectively. No such variations were noticed for specimens prepared at 8% (v/v) which gave a constant number of counts. The decrease in intensity of the various fragments presented in Figure 10 is in line with an increase of crosslink density. As the material becomes more crosslinked, with an increased number of covalent bonds between adjacent molecules, it is more difficult to produce small fragment ions by sputtering. Van Ooij and Sabata also reported the polymerisation

and crosslinking of aminosilanes upon heating, when thick films of *N*-[2-(vinylbenzylamino)-ethyl]3-amino-propyltrimethoxysilane are deposited on zinc substrates [26]. Degradation of the samples or decrease of the film thickness may also lead to the same phenomenon. Bertelsen showed that an increase in temperature produces an increase of Si–O–Si formation in a GPS film formed on aluminium, indicative of an increase in crosslink density [17]. He also showed that setting the film drying temperature at 180°C results into formation of carbonyl due to the oxidation and/or degradation of the epoxide ring. The same phenomenon was noticed at lower temperatures of 93°C and 110°C, although not as marked. This is in line with a decrease in intensity of the fragment at mass $m/z = 57$ in the ToF-SIMS spectrum and Figure 10b.

Davis and Watts used molecular modelling to predict the thickness of a monolayer of silane molecule from the epoxy end to the silanol group [6]. It was found that a thickness of 1.3 nm was monolayer coverage of silane for silane molecules standing vertically on the surface in a brush-like conformation. Table V shows the apparent thickness of GPS films for all specimens. Four specimens out of nine exhibit a thickness above that of a monolayer. The samples dried at room temperature exhibit multilayers of GPS. This is also the case of samples treated with 8% GPS solution when dried below 120°C. As argued by Davis and Watts, a structure composed of a monolayer and a random distribution of GPS molecules can be expected in the case of such samples. Increase in the crosslinking of GPS molecules among them will result in a lack of mobility, a shrinking effect [27] and may also influence the orientation of the molecules; *i.e.*, if GPS molecules are oriented at an angle of $< 90^\circ$ to the substrate, the film thickness may appear to be of the submonolayer type. Thus, “submonolayer” coverage may reveal a re-orientation of GPS molecules from perpendicular to flat on the surface or, more likely, some position in between. This is a phenomenon which is difficult to investigate on a grit-blasted surface.

Another hypothesis quoted above is the disappearance of solvents contained in the GPS film when it is subjected to high temperature drying. The expected resulting effect is again one of “shrinking” as the solvent previously swelling the film evaporates. This effect may be stopped if the film becomes too crosslinked, hindering the diffusion of the molecules and their evaporation.

5. CONCLUSIONS

A study on the effect of drying temperature on silane films has been performed using XPS and ToF-SIMS. It has been shown that:

1. Curing temperatures can be classified in two groups, below 50°C and above 93°C. It is stated that the structure of the resulting films is different in these two groups.
2. The resulting structure exhibits thicknesses varying from above monolayer to submonolayer. This is explained in terms of crosslink density, or solvent (water/methanol) removal. Assumptions were also made concerning the possible degradation of the films at high temperature.
3. This indicates that there must be an ideal temperature for which optimum interaction is obtained. This kind of film must exhibit an apparent thickness close to a monolayer (1.3 nm).
4. Contrary to expectations, initial contamination was not displaced by the adhesion promoter and remained when it was applied to the aluminium surface.

Acknowledgements

The authors thank Nigel Porrit for his help in preparing the samples. AR is grateful for a Thai Government Scholarship, MLA is a DERA/SMC Fellow.

References

- [1] Plueddemann, E. P., *Silane Coupling Agents* (Plenum Press, New York, 1991).
- [2] Digby, R. P. and Shaw, S. J., *Int. J. Adhes. Adhes.* **18**, 261 (1998).
- [3] *Silane and Other Coupling Agents*, Mittal, K. L. Ed. (VSP, Utrecht, 1992).
- [4] Bailey, R. and Castle, J. E., *J. Mater. Chem. Sci.* **12**, 2049 (1977).
- [5] Gettings, M. and Kinloch, A. J., *J. Mater. Sci.* **12**, 2511 (1997).
- [6] Davis, S. J. and Watts, J. F., *Int. J. Adhes. Adhes.* **16**, 5 (1996).
- [7] Leung, Y. L., Yang, Y. P., Wong, P. C. and Mitchell, K. A. R., *J. Mater. Sci.* **12**, 844 (1993).
- [8] Fang, J., Flinn, B. J., Leung, Y. L., Wong, P. C. and Mitchell, K. A. R., *J. Mat. Sci. Let.* **16**, 1675 (1997).
- [9] Leung, Y. L., Zhou, M. Y., Wong, P. C. and Mitchell, K. A. R., *Appl. Surf. Sci.* **59**, 23 (1992).
- [10] Abel, M.-L., Digby, R. P., Fletcher, I. and Watts, J. F., *Surf. Inter. Anal.* **29**, 115 (2000).

- [11] Osterholtz, F. D. and Pohl, E. R., *J. Adhesion Sci. Technol.* **6**, 127 (1992).
- [12] Pu, Z. C., van Ooij, W. J. and Mark, J. E., *J. Adhesion Sci. Technol.* **11**, 29 (1997).
- [13] van Ooij, W. J. and Sabata, A., *Surf. Interface Anal.* **20**, 475 (1993).
- [14] Abel, M. L., Watts, J. F. and Digby, R. P., *Int. J. Adhes. Adhes.* **18**, 179 (1998).
- [15] Woo, H., Reucroft, P. J. and Jacob, R. J., *J. Adhesion Sci. Technol.* **7**, 681 (1993).
- [16] Kuhbander, R. J. and Mazza, J. J., *Proceedings of the 38th International SAMPR Symposium*, May 10–13, p. 1225.
- [17] Bertelsen, C. M., *M.Sc. Thesis Dissertation*, University of Cincinnati (1997).
- [18] Bertelsen, C. M. and Boerio, F. J., *J. Adhesion* **70**, 259 (1999).
- [19] Abel *et al.*, unpublished results.
- [20] *Handbook of Static Secondary Ion Mass Spectrometry (SIMS)*, Briggs, D., Brown, A. and Vickerman, J. C. (Wiley, Chichester, 1989).
- [21] *Practical Surface Analysis*, Briggs, D. and Seah, M. P. Eds. (Wiley, Chichester, 1990).
- [22] Watts, J. F. and Castle, J. E., *Int. J. Adhes. Adhes.* **19**, 435 (1999).
- [23] *The Wiley Static SIMS Library*, Vickerman, J. C. and Briggs, D. (Project Directors), Henderson, A. (Project co-ordinator) (Wiley, Chichester, 1987).
- [24] Dillingham, R. G. and Boerio, F. J., in [3], pp. 493–501.
- [25] Mishra, S. and Weimer, J. J., *J. Adhesion Sci. Technol.* **11**, 337 (1997).
- [26] van Ooij, W. J. and Sabata, A., in [3], pp. 323–343.
- [27] *Polymer Handbook*, Brandrup, J., Immergut, E. H., Grulke, E., Abe, A. and Bloch, D. R. Eds. (Wiley, Chichester, 1999).